مجلة كلية التربية الاساسية

كلية التربية الاساسية – الجامعة المستنصرية

Journal of the College of Basic Education Vol.32 (NO. 136) 2026, pp. 433-451

Numerical analysis and stability of a prey-predator model with partial refuge and continuous harvesting

Sarah Ghafel(1)
Department of Networks and Computer Software
Techniques, Amarah Technical Institute, Southern Technical
University , Amarah, Basra, Iraq
sarah.ghafel@stu.edu.iq

Abstract:

A modified prey–predator model with partial refuge and proportional harvesting is investigated. The model consists of a pair of nonlinear ordinary differential equations that describe the interaction between prey and predator. The growth of the prey population is influenced describing by logistic factors and a Holling type II response. The solution is proven to exist, be positive, and be bounded. We determine all biologically feasible equilibrium points and study their local stability using the Routh-Hurwitz. For the global stability of the boundary and interior equilibrium points, the Lyapunov function construction is also used. The analytical results are validated in the numerical simulations describing the dynamical behaviour of the system.

Keywords: Prey–predator model, partial refuge, proportional harvesting, stability analysis.

Introduction:

Ecological systems often contain species competing with each other. In this predator-prey relationships placement, students will learn more about these interactions. There are limitations to the use of classical models, which rest on strong simplifications (oversimplifications). Thus, they assume unlimited growth of prey as well as linear predation. There have been many extensions proposed including logistic prey growth, non-linear functional responses, harvesting effects, and prey refuge mechanisms to overcome it. The Holling type II functional response is a well-liked model among nonlinear predation models. The model takes into consideration predator satiation and handling time. This functional response hinders predator overpopulation and improves coexistence dynamics realism. The natural ecosystems continuously fluctuate and maintain stability. According to Tewa et al. 2013 and Ma et al. 2017, that is not explained by Lotka-Volterra equations that assume linear predation and

---

unlimited growth. So, many models have been constructed and analyzed containing logistic prey growth, Holling type functional responses and other environmental mechanisms (Billiard et al., 2018, Zhang & Ma, 2018). One of the most essential predator-prey models is the Holling type II functional response which includes predator satiation and a limited handling time. The nonlinear term controls predation pressure (Liu et al., 2018; Antwi-Fordjour et al., 2020). It allows coexistence for some parameters and prevents unrealistic explosions of predators. With the addition of the influence of the refuge, the mutual interference among predators as well as fear effects substitution the structure and stability of the steady-state of the system undergoes a vast radical change which yields rich dynamic behaviour patterns like chaos, limit cycles, and bifurcation phenomena (Hossie et al., 2023; Liu Hanwu et al., 2018). In recent decades, harvesting has received. According to (Kar, 2010; Chakraborty, 2012), it is evident that the harvesting terms may significantly affect population survival and biodiversity whether they are proportionate constant or not. Bi-harvesting models which involve the simultaneous harvesting from predator and prey (Kribs-Zaleta, 2009; Liu & Huang, 2019; Lu etal, 2023) are used to study the optimal control policies and sustainable exploitation strategies. The parameter H, which denotes harvesting effort or efficiency, represents the prey and predator in these models. Theoretical and numerical investigations indicate that over-harvesting could destabilize equilibrium points, reduce resilience, or even cause species extinction (Hm.) (Sahoo et al. 2016; Mohdeb 2025.). Identifying crucial thresholds for sustainable yield can thus be an important issue for ecology. They look at how harvesting interacts with ecological effects like the Allee effect or varying predator food supplies. The behaviour of the mechanism affects the stability of global equilibrium and the extent of their coexistence. The project is inspired by how we manage real-world ecosystems so that they do not change drastically. Latest developments in mathematical modelling and bifurcation theory have allowed researchers to explore transitions between different dynamical regimes such as hopping bifurcation, and multiple equilibrium states. According to Sahoo et al (2016) and Lu et al (2023), Human activity is impacting ecological dynamics and vice versa. To summarise, the predator-prey models with multiple harvesting terms, logistic prey growth, and non-linear Holling functional response will give a more versatile tool for studying population control, stability, and sustainability under realistic economic and environmental constraints (Antwi-Fordjour et al., 2020; Liu Xinxin et al., 2019). With the help of these models, sustaining harvesting and better understanding complex ecological systems. The predator-prey system on both species with logistic growth, nonlinear interaction and harvesting pressure is a focus of the study of the local stability and bifurcation behaviour of the predator-prey system using the theoretical framework of Mohdeb (2025) and Kar (2010).

2-Model Formulation:

This part includes the methodology and how to use it. The system under consideration consists of a set of nonlinear differential equations which govern the predator $P(t)$and prey $N(t)$ population dynamics. The size of the prey's population (β) enjoys logistically growth with an intrinsic growth rate (r) and a carrying capacity (K) due to the impact of predation harvesting rate (h_1) and the refuge factor (m) which constitutes the portion. Going forward, the prey will escape. The rates of death are (d) and (h_2), which causes the predator population to diminish as the predators die and loot. Furthermore, the predator population tends to increase as they consume prey due to the conversion efficiency of (c). The term refuge modifies the functional response type II of Holling. In the model all the parameters are assumed to be positive except the $m \in [0,1)$ which is the level of protection for prey species. The model can be rewritten in a compact form through two functions $f_1(N,P)$and $f_2(N,P)$ for equilibrium points (EP) analysis and their stability properties.

$$\frac{dN}{dt} = rN\left(1 - \frac{N}{K}\right) - \frac{\alpha(1-m)NP}{1+\beta(1-m)N} - h_1 N$$

(2.1)

$$\frac{dP}{dt} = P\left(\frac{c\alpha(1-m)N}{1+\beta(1-m)N} - d\right) - h_2 P$$

Parameter	Description
N	Rate of prey
P	density of predators
r	Intrinsic growth rate
K	Ability to transport
$m \in [0,1)$	Prey refuge proportion: the percentage of prey that is shielded from predators
β	Handling time parameter
α	Attack rate
c	Conversion efficiency

d	Natural death rate
$h_1 \geq 0$	Prey harvesting
$h_2 \geq 0$	Predator harvesting rate

Theorem (2.1): For system (2.1), the region $R_+^2 = \{(N,P) \in R^2 : N \geq 0, P \geq 0\}$ is positively invariant.

Proof: Both functions $f_1(N,P)$and $f_2(N,P)$ are differentiable within the first quadrant due to their construction as composite of rational plus polynomial functions having positive denominators. This means that Lipschitz conditions in the open quarter plane guarantee the existence and uniqueness of the solution $(N(t),P(t))$with any positive initial condition.

For the N-axis $(N=0)$: from the first equation of the system

$$\dot{\mathrm{N}}\Big|_{\mathrm{N}=0} = \mathrm{r}(0)\left(1-\frac{0}{K}\right)-\frac{\alpha(1-m)(0)P}{1+\beta(1-m)(0)}-h_1(0)=0$$

This implies that the N-axis is an invariant manifold; if a trajectory starts with $N(0) > 0$, it can never $N = 0$ cross the line

For the P-axis $(P=0)$: from the first equation of the system

$$\dot{P}\Big|_{P=0} = 0[\frac{c\alpha(1-m)N}{1+\beta(1-m)N}-(d+h_2)]=0$$

$$\dot{P}\Big|_{P=0} = 0 \rightarrow P(t) \geq 0$$

Similarly, this implies that the P-axis is invariant

Since the axes are invariant and the solution are unique, any trajectory starting in the interior of the first quadrant $t > 0$ R_+^2 will remain in R_+^2 for all.

Theorem (2.2): All solutions $(N(t),P(t))$ of system (2.1) starting from $\{R_+^2 - \{0\}\}$ are uniformly confined.

Proof: Let $B(t)$be the size of the system (2.1), $B(t) = N(t) + \frac{1}{c}P(t).N(t) and\, P(t)$ can be chosen to be arbitrary solutions of system (2.1). $B(t)$ is bounded if and only if $N(t)$ and $P(t)$ are bounded.

The time derivative of $B(t)$

$$\dot{B} = \dot{N} + \frac{1}{c}\dot{P}$$

$$\dot{B} = rN\left(1-\frac{N}{K}\right)-\frac{\alpha(1-m)NP}{1+\beta(1-m)N}-h_1N+\frac{1}{c}[P\left(\frac{c\alpha(1-m)N}{1+\beta(1-m)N}-d\right)-h_2P]$$

$$\dot{B} \leq rN-\frac{r}{K}N^2-dP \leq M-\delta(N+P)$$

$$\lim sup_{t\to\infty}(N(t)+P(t)) \le \frac{M}{\delta}$$

3. The presence of equilibrium points

In this section, we study the local stability of a non-autonomous system of ODEs. Using linearization techniques the dynamic behavior of a highly complex non-linear system with three physiologically important equilibrium points is demonstrated. After we linearize the equations around each equilibrium point, and make a small perturbation, we check whether the system returns.

(i) The trivial equilibrium point always exists in every dynamical system$\Lambda_0 = (\bar{N}, 0)$, where $\bar{N} = K\left(1-\frac{h_1}{r}\right), r > h_1$.

(ii) The axial equilibrium point (AEP) Λ_1 can be computed using standard results. Using the limits $\bar{N} \to 0$, the use of $\bar{N} = K(1-\frac{h_1}{r})$, where $r > h_1$.

(iii) The internal equilibrium point IEP is given by$\Lambda_2 = (N^*, P^*)$.

We subsequently discuss the existence of an interior equilibrium $\Lambda_2$where the values of N^*, P^* may be obtained by solving the following set of algebraic equations.

From equation (2)

$$N^* = \frac{d+h_2}{(1-m)[\alpha c - \beta(d+h_2)]}$$

$$c\alpha > \beta(d+h_2), N^* < K$$

So,

$$P^* = \frac{1+\beta(1-m)N^*}{\alpha(1-m)}[r\left(1-\frac{N^*}{K}\right)-h_1]$$

By condition

$$c\frac{\alpha(1-m)N^*}{1+h(1-m)N^*} > d+h_2$$

4. Local Stability Analysis:

An assessment of local stability can predict the future evolution of a system. For this reason, we elaborate on the equilibrium points EP i=1,2. The conditions for stability and instability. The linearization of system about any point (EP) gives the following form of the variational matrix.

$$J=\begin{bmatrix} r\left(1-\frac{2N}{K}\right)-\frac{\alpha(1-m)P}{(1+\beta(1-m)N)^2}-h_1 & -\frac{\alpha(1-m)N}{1+\beta(1-m))N} \\ P\frac{c\alpha(1-m)}{[1+\beta(1-m)N]^2} & \frac{c\alpha(1-m)N}{1+\beta(1-m)N}-d-h_2 \end{bmatrix} \qquad (4.1)$$

Eigenvalues at local stability points (EP) are defined as follows.

Theorem (4.1): The system (2.1) with (TEP) $\Lambda_0=(0,0)$ is usually an unstable saddle point.

Proof: The mutation matrix (4.1) in (TEP) is given as.

$$J_{\Lambda_0}=\begin{bmatrix} r-h_1 & 0 \\ 0 & -d-h_2 \end{bmatrix} \qquad (4.2)$$

$\lambda_1=r-h_1>0, \lambda_2=-(d+h_2)<0$

Is a saddle unstable point

Theorem (4.2) A system (2.1) around an (AEP)$\Lambda_1=(\bar{N},0)$, if it satisfies the below conditions it is said to be locally asympathically stable.

$\frac{c\alpha(1-m)N_1}{1+h(1-m)N_1}<d+h_2$

Proof: The matrix of variation near AEP is as follows:

$$J_{\Lambda_1}=\begin{bmatrix} r(1-\frac{2\bar{N}}{K}) & -\frac{\alpha(1-m)\bar{N}}{1+\beta(1-m)\bar{N}} \\ 0 & \frac{c\alpha(1-m)\bar{N}}{1+\beta(1-m)\bar{N}}-d-h_2 \end{bmatrix} \qquad (4.3)$$

Thus, the characteristic polynomial of the matrix J_{Λ_1} is given as.

$$[\ r\left(1-\frac{2\bar{N}}{K}\right)-\lambda_1][\left(\frac{c\alpha(1-m)\bar{N}}{1+\beta(1-m)\bar{N}}-d-h_2\right)-\lambda_2]$$

The conditions given below are sufficient for AEP to be an asymptotically stable local equilibrium point of system (2.1).

- $\lambda_1=r(1-\frac{2\bar{N}}{K})<0$
- $\lambda_2=\frac{c\alpha(1-m)\bar{N}}{1+\beta(1-m)\bar{N}}-d-h_2<0$ ■

Theorem (4.3): Assume that:

- $Tr\left(J(\Lambda_2)\right)<0,\ Det(J(\Lambda_2))>0$

If T and D are defined as in the proof, then (IEP) $\Lambda_2=(N^*,P^*)$ is locally stable for the system (2.1).

Proof: The matrix of variation close to (IEP) is described as follows.

$$J_{\Lambda_2}=\left(W_{ij}\right)_{2\times2} \qquad (4.4)$$

Where,

$$W_{11}^*=r\left(1-\frac{2N^*}{K}\right)-\frac{\alpha(1-m)p^*}{[1+\beta(1-m)N^*]^2}-h_1$$

$$W_{12}^* = -\frac{\alpha(1-m)N^*}{1+\beta(1-m)N^*}$$

$$W_{21}^* = P^*\frac{c\alpha(1-m)}{[1+\beta(1-m)N^*]^2}$$

$$W_{22}^* = \frac{c\alpha(1-m)N^*}{1+\beta(1-m)N^*} - d - h_2$$

Evaluating a characteristic equation of J_{Λ_2}, gives

$$\lambda^2 + T\lambda + D = 0 \qquad (4.5)$$

where

$$T = W_{11}^* + W_{22}^*\ , D = W_{11}^* W_{22}^* - W_{12}^* W_{21}^*$$

In order for condition (4.5) to have all roots with negative real parts, the conditions are: $T < 0, D > 0, W_{11}^* < 0$Consequently, Λ_2 is stable at the local level. ■

5-The Analysis of Global Stability

In this section, the Lyapunov method is used to analyses the global stability of system (2.1) (EP) (LAS).

Theorem (5.1): The system (2.1) $\Lambda_1 = \left(K\left(1-\frac{h_1}{r}\right), 0\right)$ is said to be globally stable whenever it is locally stable and (AEP) satisfies the following condition.

- $\frac{c\alpha(1-m)N^*}{1+\beta(1-m)N} \le \frac{c\alpha(1-m)N^*}{1+\beta(1-m)N^*}$
- $\frac{\alpha(1-m)N_1}{1+\beta(1-m)N} < \frac{d+h_2}{c}$
- $\dot{V}_1 \le -\frac{r}{K}(N-N^*)^2 < 0, \forall(N,P) \ne \Lambda_1$

Proof: Think about the following function

$$V_1(V,P) = N - N_1^* - N_1^* ln\frac{N}{N_1^*} + \frac{1}{c}P$$

$$\dot{V}_1 = \frac{N-N_1^*}{N}\dot{N} + \frac{1}{c}\dot{P}$$

$$\dot{V}_1 = \frac{N-N_1^*}{N}\left[rN\left(1-\frac{N}{K}\right) - \frac{\alpha(1-m)NP}{1+\beta(1-m)N} - h_1 N\right]$$

$$+\frac{1}{c}[P\left(\frac{c\alpha(1-m)N}{1+\beta(1-m)N} - d\right) - h_2 P]$$

$$\dot{V}_1 = (N-N_1)\left[-\frac{r}{K}(N-N_1) - \frac{\alpha(1-m)P}{1+\beta(1-m)N}\right] + \frac{\alpha(1-m)NP}{1+\beta(1-m)N} - \frac{d+h_2}{c}P$$

$$\dot{V}_1 = -\frac{r}{K}(N-N_1)^2 - \frac{\alpha(1-m)P(N-N_1)}{1+\beta(1-m)N} + \frac{\alpha(1-m)NP}{1+\beta(1-m)N} - \frac{d+h_2}{c}P$$

$$\dot{V}_1 \le -\frac{r}{K}(N-N_1)^2 + P[\frac{\alpha(1-m)N_1}{1+\beta(1-m)N} - \frac{d+h_2}{c}]$$

It is clearly to see: $V_1(N,P) \in c^1(R_+^3,R)$, $v_1(\Lambda_1) = 0$, and $V_1(N,P) > 0$; $\forall (N,P) \neq \Lambda_1$. Hence V_1 is a Lyapunov function. Therefore, Λ_1 is globally asymptotically stable in R_+^3. ■

Theorem (5.2): The global asymptotic stability of the (IEP) $\Lambda_2 = (N^*, P^*)$ of system (2.1) holds if:

- $V_2(\Lambda_2) = 0$
- $V_2(N,P) > 0 \; for \; all \; (N,P) \neq \Lambda_2$
- $V_2 \in C^1(R_+^2)$

Proof: First, a Lyapunov function may be define as:

$$V_2(N,P) = \left(N - N^* - N^* ln\frac{N}{N^*}\right) + \frac{1}{c}(P - P^* - P^* ln\frac{P}{P^*})$$

$$\dot{V}_2 = \left(1 - \frac{N^*}{N}\right)\dot{N} + \frac{1}{c}(1 - \frac{P^*}{P})\dot{P}$$

$$\dot{V}_2 = \left(1 - \frac{N^*}{N}\right)\left[rN\left(1 - \frac{N}{K}\right) - \frac{\alpha(1-m)NP}{1+\beta(1-m)N} - h_1 N\right] + \frac{1}{c}\left(1 - \frac{P^*}{P}\right)[P\left(\frac{c\alpha(1-m)N}{1+\beta(1-m)N} - d\right) - h_2 P]$$

$$\dot{V}_2 = (N-N^*)\left[-\frac{r}{K}(N-N^*) - \left(\frac{\alpha(1-m)P}{1+\beta(1-m)N} - \frac{\alpha(1-m)P^*}{1+\beta(1-m)N^*}\right)\right] + (P-P^*)[\frac{\alpha(1-m)N}{1+\beta(1-m)N} - \frac{\alpha(1-m)N^*}{1+\beta(1-m)N^*}]$$

$$\dot{V}_2 \le -(N-N^*)^2[\frac{r}{K} - \frac{\alpha\beta(1-m)^2P^*}{(1+\beta(1-m)N)(1+\beta(1-m)N^*)}]$$

condition $\frac{dV_2}{dt} \le 0$. This means $V_2(N,P)$ is negative definite is globally stable. Moreover, $\frac{dV_2}{dt} = 0$ if and only. Therefore, due the LaSalle theorem, (IEP) is global asymptotically stable and this completes the proof. ■

6-Local Bifurcation Analysis:

Let $X = (N,P)^T$, $\dot{X} = F(X,\mu)$

Theorem (6.1): the model at A axial equilibrium point (AEP) have transcritical bifurcation occurs at $m = m_c$

Proof:

Jacobian at Λ_1

$$J(\Lambda_1) = \begin{bmatrix} r(1-\frac{2N_1}{K}) - h_1 & \frac{-\alpha(1-m)N_1}{1+\beta(1-m)N_1} \\ 0 & \frac{c\alpha(1-m)N_1}{1+\beta(1-m)N_1} - d - h_2 \end{bmatrix}$$

Bifurcation condition $\lambda_2 = 0 \ \rightarrow m = m_c$

Eigenvectors $v = (1,0)^T$, $w = (0,1)^T$

Transversality $\frac{d\lambda_2}{dm} = -\frac{c\alpha N_1}{[1+\beta(1-m_c)N_1]^2} \neq 0$

Nondegeneracy $w^T D^2 F(\Lambda_1)(v,v) = -\frac{2c\alpha\beta(1-m_c)^2 N_1}{[1+\beta(1-m_c)N_1]^3} \neq 0$

Conclusion: A transcritical bifurcation occurs at $m = m_c$

Theorem (6.2): the model (2.1) at An interior equilibrium point (IEP) have a Hopf-bifurcation.

At Λ_2 ,$Tr(J) = 0$,$\det(J) > 0$

That is $r\left(1 - \frac{2N^*}{K}\right) - h_1 - \frac{\alpha(1-m)P^*}{[1+\beta(1-m)N^*]^2} = 0$

Let $\mu = m$ be the bifurcation parameter

Hopf condition $Tr\big(J(\Lambda_2)\big) = 0$,$\frac{d}{d\mu} Tr(J(\Lambda_2)) \neq 0$

Transversality $\frac{d}{dm} Re\big(\lambda_{1,2}\big) \neq 0 \ \ when\, m = m_h$

Conclusion: the coexistence equilibrium undergoes a Hopf bifurcation.

7. Numerical Simulation

We performed numerical experiments using MATLAB(which is bases on the adaptive Runge-Kutta) to illustrate the results of the analysis. The local stability of the equilibrium point was show using time series, whereas global stability was show using phase diagrams. The figures also show the effect of harvest and return parameters on the system.

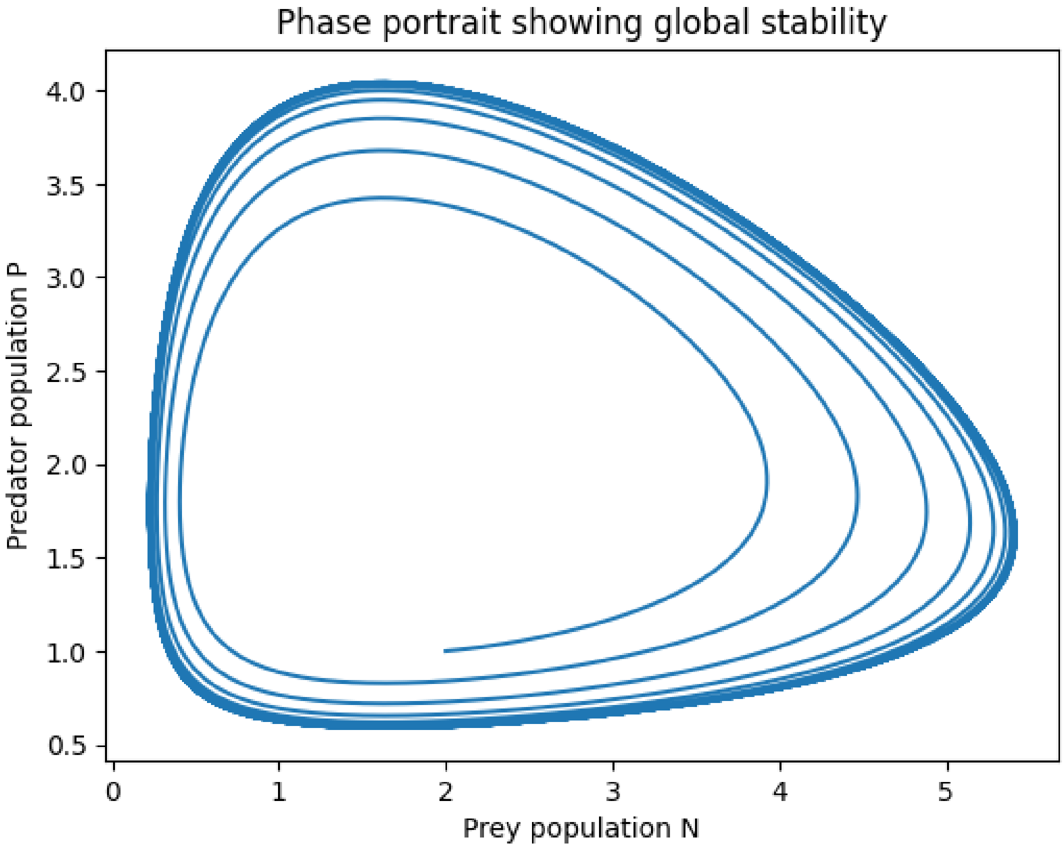

Figure: The populations of the prey and the predator are shown over time to converge to the equilibrium point confirming local stability.

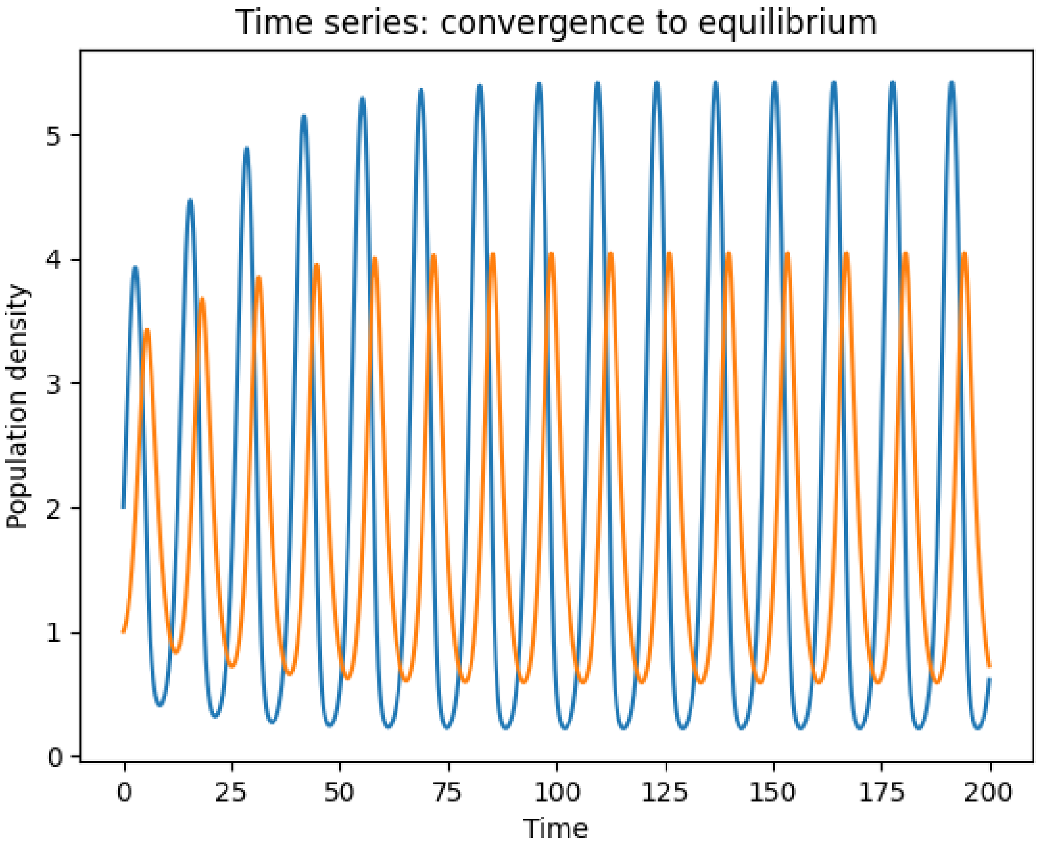

Figure 2: The system's phase portrait illustrates the equilibrium point's global stability.

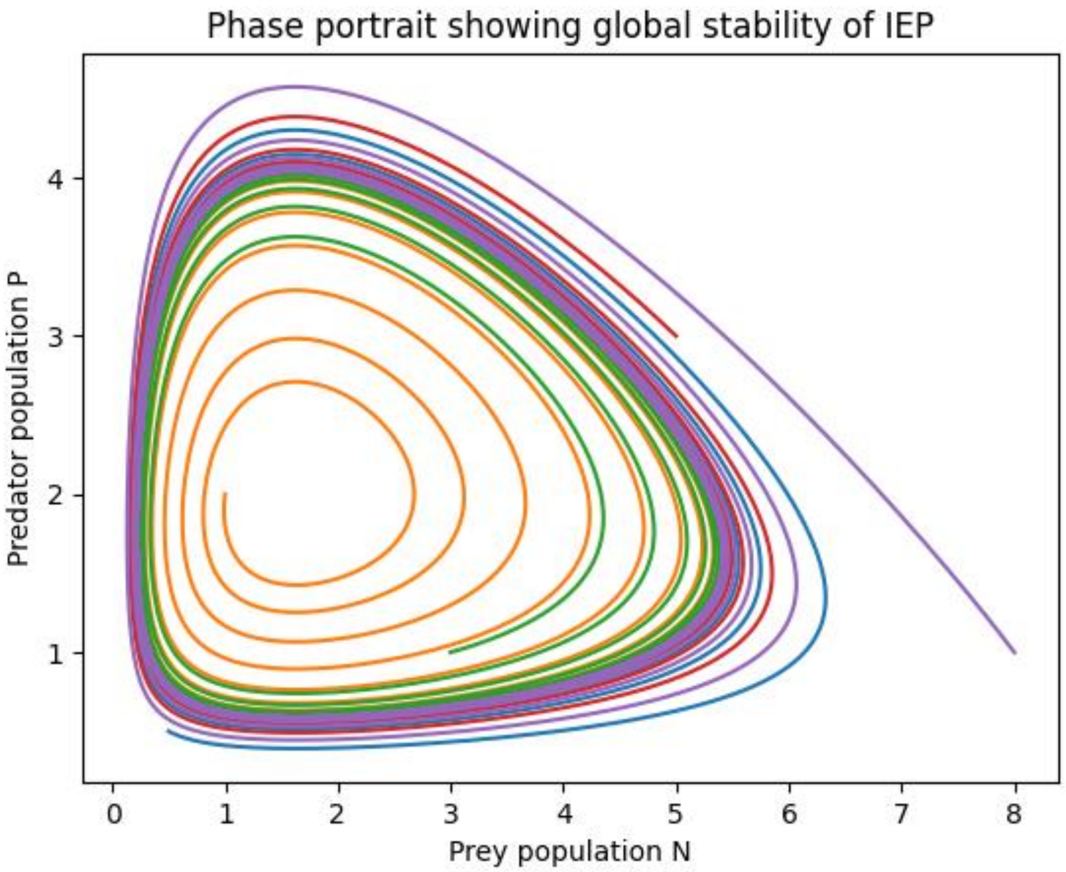

Figure 3: The graph shows the time series of prey and predator populations for initial conditions chosen close to the interior equilibrium point. Experiencing both oscillations before attaining steady states is noticed in both the populations. This verifies the interior equilibrium point’s local asymptotic stability in line with the linear stability analysis using the Routh–Hurwitz criteria.

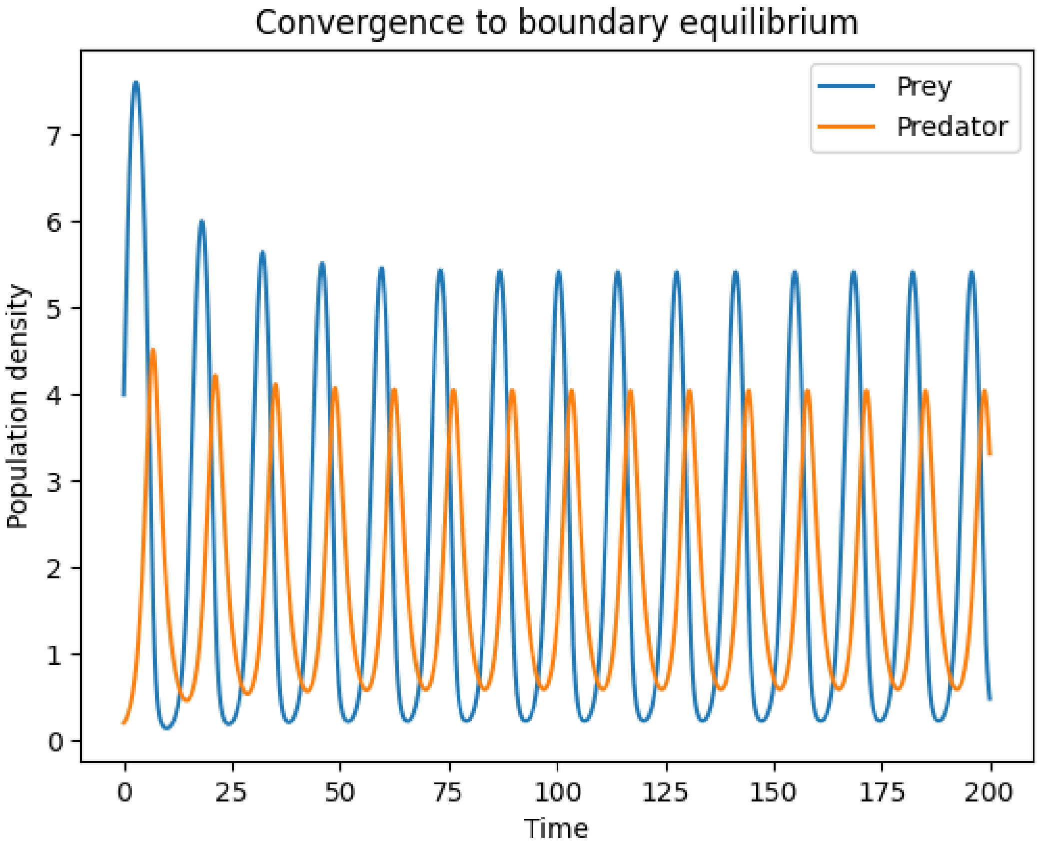

Figure 4: It shows the phase portrait of the system for three different initial conditions in the positively invariant domain. no matter the starting population sizes, all paths converge toward the same interior equilibrium point. This behavior significantly illustrates that the interior equilibrium in question is globally asymptotically stable, coinciding with the Lyapunov-based analytical results in Section 6.

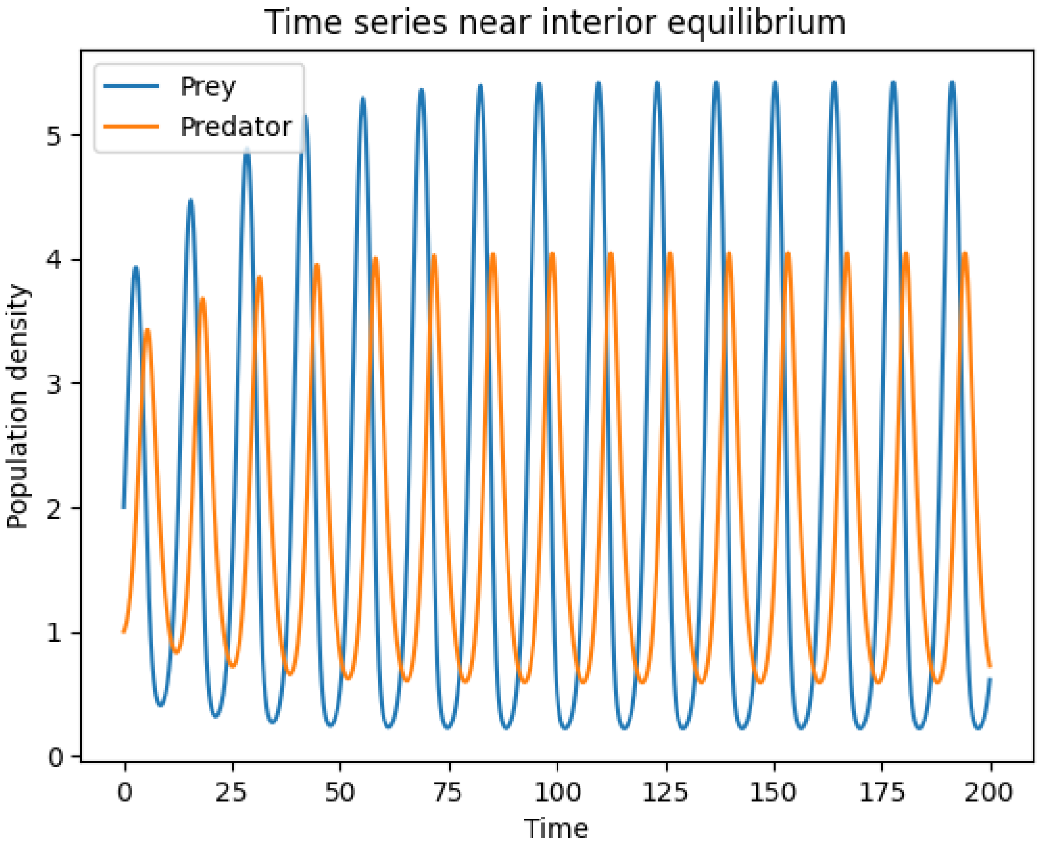

Figure 5: Shows how convergence takes place towards the boundary equilibrium point when parameter conditions prevent persistence of the predator population The numerical solution indicates that the density of the predator approaches zero asymptotically while the density of the prey stabilizes at the boundary equilibrium. The result of the present work confirms the theoretical condition of global stability of the axial equilibrium. It also indicates that harvesting pressure and refugee proportion have large impact on species survival.

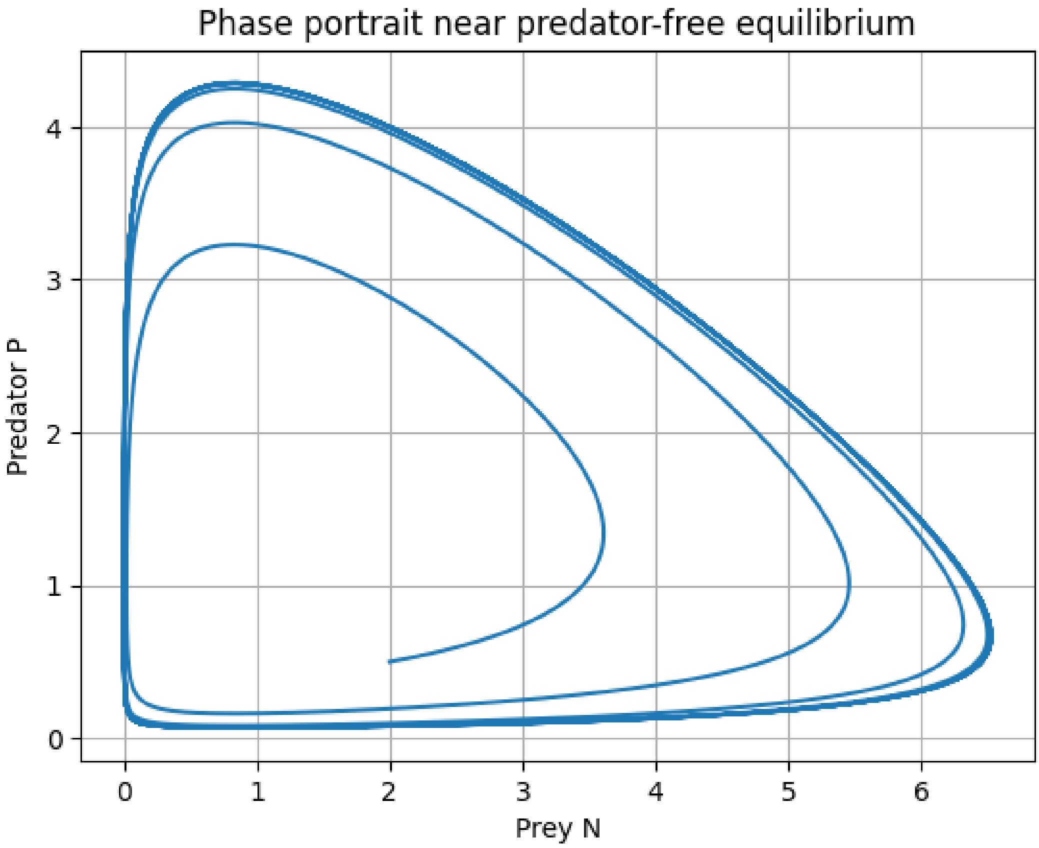

Figure 6: The predator-free equilibrium phase portrait shows the extinction of predators, and the trajectories converge toward the prey-only axis..

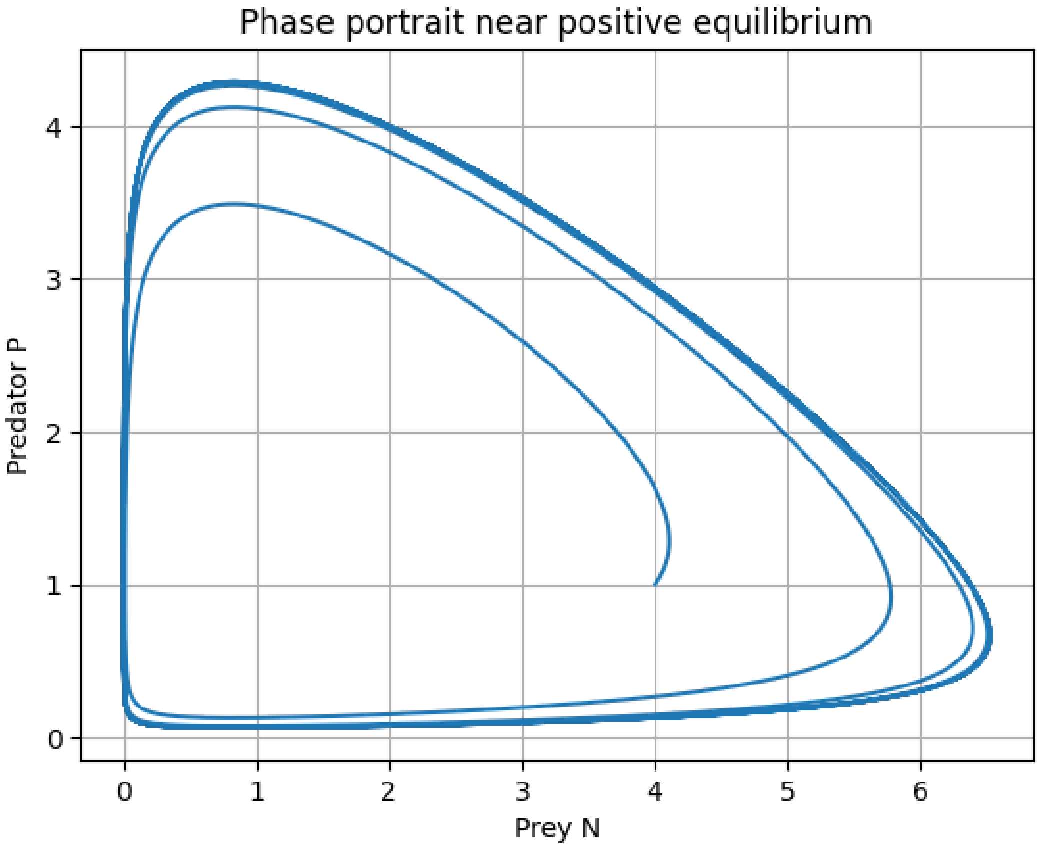

Figure 7: Illustrates the phase portrait in the neighborhood of the coexistence equilibrium, which agrees with the analytical stability results and indicates oscillatory behaviour.

Conclusion:

Analysis was conducted on a prey–predator model with partial prey refuge and proportional harvesting. The system's stability, boundedness and positivity properties are established. The results indicate that suitable harvesting strategies and refuge levels lead to coexistence and stability, while excessive harvesting may lead to trigger extinction.

Further Work

The proposed model can help in studying sustainable ecological management and it can further be expanded to include optimal harvesting strategies.

References

1. Antwi-Fordjour, K., Parshad, R.D. and Beauregard, M.A. (2020), "Dynamics of a predator–prey model with generalized Holling type functional response and mutual interference", Mathematical Biosciences, Vol. 326, Article 108407.
2. Billiard, S., Bansaye, V. and Chazottes, J.-R. (2018), "Rejuvenating functional responses with renewal theory", Journal of The Royal Society Interface, Vol. 15 No. 146, Article 20180239.
3. Chakraborty, S., Pal, S. and Bairagi, N. (2012), "Predator–prey
4. interaction with harvesting: mathematical study with biological ramifications", Applied Mathematical Modelling, Vol. 36 No. 9, pp. 4044–4059.
5. Hossie, T.J. and Murray, D.L. (2023), "New perspectives and emerging directions in predator–prey functional response research: hommage to C.S. Holling (1930–2019)", Frontiers in Ecology and Evolution, Vol. 11, Article 1238953.
6. Kar, T.K. and Chattopadhyay, S.K. (2010), "A focus on long-run sustainability of a harvested prey–predator system in the presence of alternative prey", Comptes Rendus Biologies, Vol. 333 Nos. 11–12, pp. 841–849.
7. Kribs-Zaleta, C.M. (2009), "Sharpness of saturation in harvesting and predation", Mathematical Biosciences and Engineering, Vol. 6 No. 4, pp. 719–742.
8. Liu, H., Li, T. and Zhang, F. (2018), "A prey–predator model with Holling II functional response and the carrying capacity of predator depending on its prey", Journal of Applied Analysis and Computation, Vol. 8 No. 5, pp. 1464–1474.
9. Liu, X. and Huang, Q. (2019), "Comparison and analysis of two forms of harvesting functions in the two-prey and one-predator model", Journal of Inequalities and Applications, Vol. 2019 No. 1, Article 307.

10. Liu, X. and Huang, Q. (2020), “Analysis of optimal harvesting of a predator–prey model with Holling type IV functional response”, Ecological Complexity, Vol. 42, Article 100816.
11. Lu, C.C., Liu, X.X. and Li, Z.C. (2023), “The dynamics and harvesting strategies of a predator–prey system with Allee effect on prey”, Mathematics, Vol. 8 No. 12, pp. 28897–28925.
12. Ma, Z., et al. (2017), “Stability analysis of prey–predator system with Holling type functional response and prey refuge”, Advances in Difference Equations, Vol. 2017 No. 1, Article 243.
13. Mohdeb, N. (2025), “A dynamic analysis of a prey–predator population model with a nonlinear harvesting rate”, Arab Journal of Mathematical Sciences, Vol. 31 No. 1, pp. 47–60.
14. Sahoo, B., Das, B. and Samanta, S. (2016), “Dynamics of harvested predator–prey model: role of alternative resources”, Modeling Earth Systems and Environment, Vol. 2 No. 3, Article 140.
15. Tewa, J.J., Djeumen, V.Y. and Bowong, S. (2013), “Predator–prey model with Holling response function of type II and SIS infectious disease”, Applied Mathematical Modelling, Vol. 37 No. 7, pp. 4825–4841.
16. Zhang, J.F., et al. (2018), “Optimal experimental design for predator–prey functional response experiments”, Journal of The Royal Society Interface, Vol. 15 No. 144, Article 20180186.

مجلة كلية التربية الاساسية
كلية التربية الاساسية – الجامعة المستنصرية

Journal of the College of Basic Education **Vol.32 (NO. 136) 2026, pp. 433-451**

التحليل العددي واستقرار نموذج المفترس والفريسة مع اللجوء الجزئي والحصاد المستمر

أسم سارة فوزي غافل (1)
مكان العمل الجامعة التقنية الجنوبية/ المعهد التقني العمارة/
قسم شبكات وبراميجيات الحاسوب
رقم الهاتف: 07716267263

sarah.ghafel@stu.edu.iq

مستخلص البحث:

نموذج معدل للمفترس والفريسة مع ملجا جزئي ستتم مناقشة اللجوء والحصاد النسبي. يتكون النموذج من زوج من المعادلات التفاضلية العادية غير الخطية التي تصف التفاعل بين الفريسة والمفترس. يتاثر نمو تعداد الفرائس بعوامل لوجستية واستجابة من النوع الثاني لهولينك ثبت ان الحل موجود و موجب ومحدد نحدد جميع نقاط التوازن الممكنة بيولوجيا وندرس استقرارها المحلي باستخدام متراجحات رواث-هرويتز. بالنسبة للاستقرار العالمي لنقاط التوازن الحدودية والداخلية، يتم ايضا للاستقرار العالمي لنقاط التوازن الحدودية والداخلية، يتم ايضا استخدام بناء دالة ليابونوف. يتم التحقق من صحة النتائج التحليلية في المحاكاة العددية التي تصف السلوك الديناميكي للنظام.

الكلمات المفتاحية : نموذج الفريسة والمفترس، اللجوء الجزئي ، الحصاد النسبي، تحليل الاستقرار.

ملاحظة : هل البحث مستل من رسالة ماجستير او اطروحة دكتوراه ؟ **كلا :**